

Computational fluid dynamic analyses of catalytic combustors for 100 kW-class molten carbonate fuel cell

Hai-Kyung Seo^{*†}, Donghoon Shin^{**}, Jae Hwa Chung^{*}, Beomjoo Kim^{***}, Soo Man Park^{***}, and Hee Chun Lim^{***}

^{*}Integrated Gasification Combined Cycle Group, Korea Electric Power Research Institute, 103-16, Munji-dong, Yuseong-gu, Daejeon 305-380, Korea

^{**}School of Mechanical & Automotive Engineering, Kookmin University, 861-1, Jeongneung-dong, Seongbuk-gu, Seoul 136-702, Korea

^{***}Renewable Energy Research Group, Korea Electric Power Research Institute, 103-16, Munji-dong, Yuseong-gu, Daejeon 305-380, Korea

(Received 8 August 2007 • accepted 13 July 2008)

Abstract—The asymmetric inner structure of a catalytic combustor causes wall cracking because of regional overheating. Thus, a symmetric shape is proposed in the present work and analyses of the computational fluid dynamics of the existing combustor and the proposed type have been performed. A simulation of the revised combustor without a swirl device revealed that the flow of gases is concentrated on the center of the combustor and only catalysts around the center are used. In the revised combustor with a swirl device, the overall temperatures were estimated to be uniform. However, near the swirl device, high temperature exceeding 1,700 K was measured. Therefore, a heatproof surface coating on the swirl device is necessary for protection of the material. At the initial start-up of the catalytic combustor, hydrogen and natural gas are used. When only natural gas is used, the simulation indicated that the gas does not burn in the revised combustor without a swirl device. However, in the combustor with the swirl device, methane of 34.8% volume burns in the simulation. On the other hand, when hydrogen and natural gas are burned together, methane of 91.7% volume burns in the simulation.

Key words: Catalytic Combustor, Asymmetric Structure, CFD, Swirl Device, Anode Off Gases

INTRODUCTION

The catalytic combustor in fuel cells is an important unit for efficient use of the unused fuel of the anode off gas. A catalytic combustor is used instead of a burner primarily for the following two reasons. First, the anode off gas is not an inflammable fuel, because it has less hydrogen and CO and abundant CO₂, thus reducing its flammability. To render the anode off gas combustible, a catalyst for combustion is used [1]. The other reason for using a catalytic combustor is to lessen NO_x emission, which is produced at the zone of high temperatures in a burner [2,3].

A configuration of a molten carbonate fuel cell (MCFC) system is represented in Fig. 1. In Fig. 1, DC-103 denotes the catalytic combustor. The inner structure of the existing catalytic combustor and an explanation of the numbers are described in Fig. 2. The compositions and flow rates of the anode off gas, the cathode off gas, and air inserted into the catalytic combustor are also given in Table 1. When initially heating the catalytic combustor, H₂, Natural Gas (NG), and air are used. If the temperature of the combustor reaches 400 °C, the anode off gas and cathode off gas are used.

During initial start-up, the outer metal of the catalytic combustor ruptured due to overheating. Thermocouples were located at the center and downstream of the catalyst layer, and the combustion state was monitored with these two thermocouples. Because the temperatures measured with the thermocouples appeared lower than 700 °C, the operation was continued. After rupture of the outer mate-

rial of the combustor, the computational fluid dynamics (CFD) was studied in order to assess the cause.

In this paper, through a CFD of the existing catalytic combustor, it was verified that the distribution of the inside temperature of the catalytic combustor was not uniform. Therefore, as an alternative configuration, a catalytic combustor having a symmetric inner space was proposed and a CFD analysis of the proposed combustor was conducted. The results of the CFD analyses were then compared.

In the existing catalytic combustor, each CFD analysis was performed according to the operating conditions given in Table 1. The CFD analyses of the alternative combustor were then performed with and without application of a swirl device.

In Table 1, the lower heating values of fuels are also shown. Among the four cases of operating conditions, the heat and mass balance of the case 4 is represented in Fig. 3. In Table 2, the gas compositions of each pipe in Fig. 3 are shown. The pipe where the fuel, that is, anode off gas was inserted is represented as number 2 and the condition of fuel is shown at the end of pipe, displaying pressure, temperature, enthalpy and mass flow in Fig. 3. In this calculation, the temperature of flue gas exhausted in this combustor is estimated as 660.47 °C, the mass flow is 0.413 kg/s and the gas compositions of each pipe are shown in Table 2. This calculation was performed by using the Cycle-Tempo 5.0 program. The combustion reactions are shown in Table 3.

MATHEMATICAL MODEL

The thermal flow phenomena inside the catalytic combustor include turbulence, heat transfer, and volumetric chemical reactions.

[†]To whom correspondence should be addressed.
E-mail: seohk@kepri.re.kr

100kW Externally Reforming MCFC Power Generation System

Fuel gas : Externally Reformed Syn gas
 MCFC Stack : 0.6 m², 170ea, Co-flow type.
 Operation Condition : 1-7kg/cm², 650°C
 U_f=0.8, U_{ox}=0.3, 0.8V, 125mA/cm²

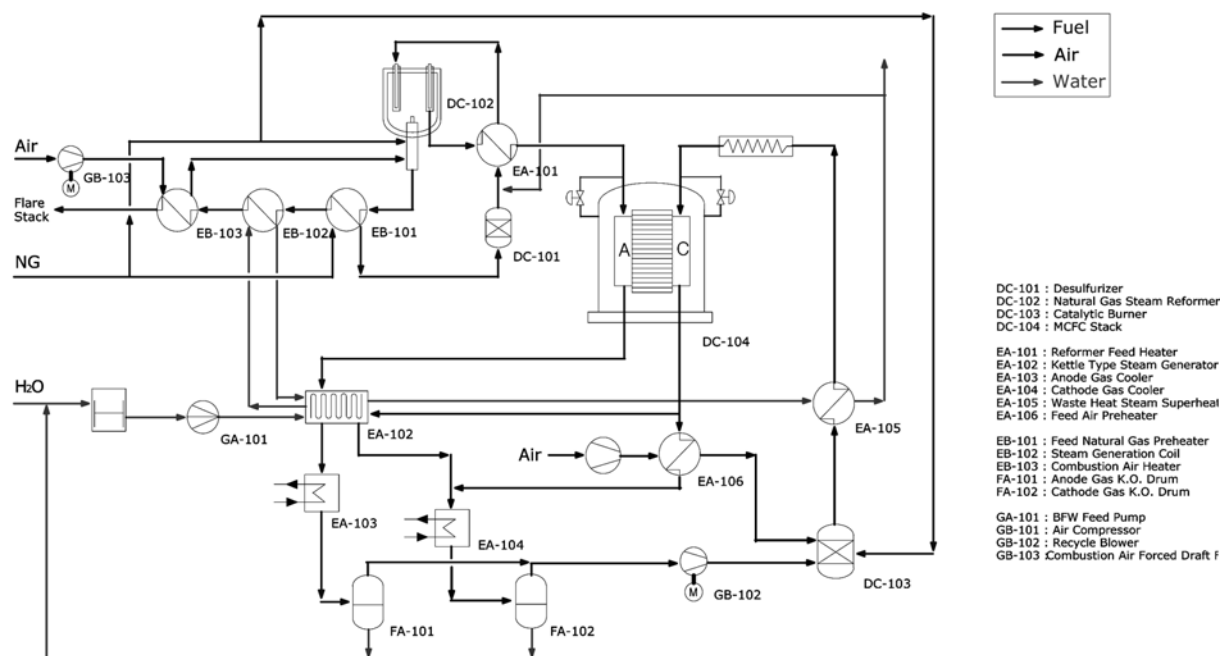


Fig. 1. Configuration of a 100 kW-class MCFC system.

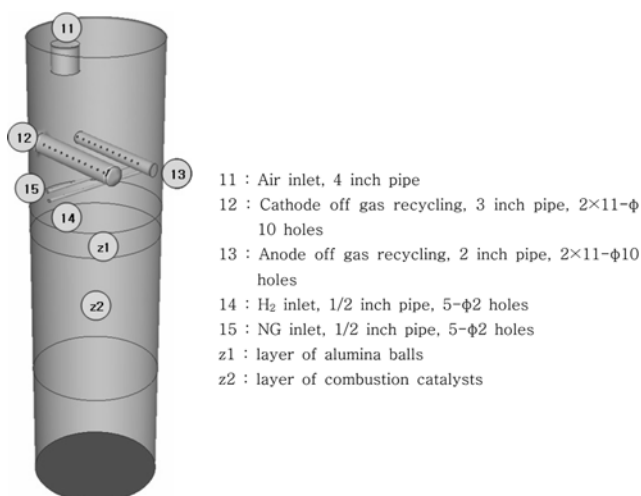


Fig. 2. Inner structure of the existing catalytic combustor.

A commercial computational fluid dynamics code, FLUENT V.6.2, is applied to analyze the phenomena [4]. The turbulence model is the standard k-ε model [5], which requires an economical calculation load and provides reasonable accuracy for a chemical reacting flow. The reaction model is a volumetric reaction controlled by competition between an Arrhenius type finite-rate reaction and the eddy-dissipation rate [6]. The considered reactions and their reaction coefficients are listed in Table 3.

The flow resistance by the porous media of the catalyst layer is

considered as a source term in the flow momentum equation as follows:

$$\frac{\partial}{\partial t}(\rho \vec{v}) + \nabla \cdot (\rho \vec{v} \vec{v}) = -\nabla p + \rho \vec{g} + \vec{S}$$

The i-components of the source term \vec{S} by the porous media are as follows [7]:

$$S_i = -\left(\frac{\mu}{\alpha} + C_2 \frac{1}{2} \rho v_{mag} v_i\right)$$

$$\alpha = \frac{D_p^2}{150} \frac{\varepsilon^3}{(1-\varepsilon)^2}$$

$$C_2 = \frac{3.5(1-\varepsilon)}{D_p \varepsilon^3}$$

Here, α is the permeability, ε is the void fraction of the porous media, C_2 is the inertial loss factor of the porous media, μ is the viscosity of the fluid, and D_p is the diameter of the catalyst. In the present study, the void fraction ε is 0.4 and the diameter of the catalyst D_p is 4 mm.

RESULTS AND DISCUSSION

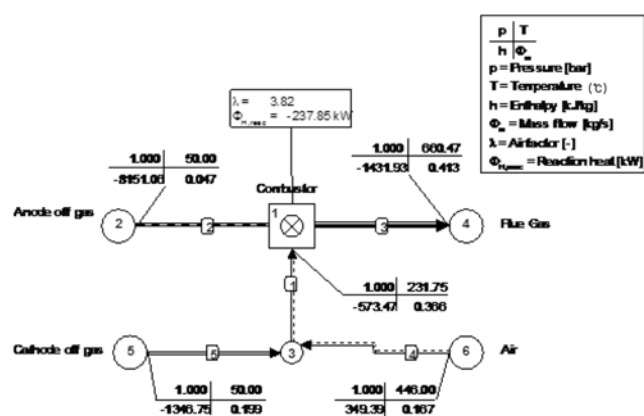
1. CFD Analysis of the Existing Catalytic Combustor

The specifications of the catalyst in the existing catalytic combustor are presented in Table 4.

For the design of the combustor, the gas hourly space velocity (GHSV) passing through the catalyst layer was assumed to be about 10,000 hr⁻¹ at normal operating conditions and the diffusion of fuel

Table 1. Operating conditions of the catalytic combustor for CFD analysis

Flow rate (Nm ³ /h), Temperature (°C)	Case 1		Case 2		Case 3		Case 4	
	Flow rate	Temp	Flow rate	Temp	Flow rate	Temp	Flow rate	Temp
Air	200	180	200	180	200	180	467	446
Cathode off gas	0	0	0	0	0	0	551.2	50
Anode off gas	0	0	0	0	0	0	136.8	50
H ₂ (when initial heating)	5	20	0	0	5	20	0	0
NG (when initial heating)	0	0	5	20	5	20	0	0
Composition of Cathode off gas (v/v%)	O ₂ 6.6%, N ₂ 81.8%, CO ₂ 7.9%, H ₂ O 3.7%							
Composition of Anode off gas (v/v%)	H ₂ 30.9%, CO 12.1%, CO ₂ 51.4%, CH ₄ 2.0%, H ₂ O 3.6%							
lower heating value of H ₂	2,560.9 kcal/Nm ³ , 57,364.2 kcal/kgmole							
lower heating value of CH ₄	8,531.0 kcal/Nm ³ , 191,094.4 kcal/kgmole							
lower heating value of CO	3,014.0 kcal/Nm ³ , 67,513.6 kcal/kgmole							
lower heating value of Anode off gas	1,326.6 kcal/Nm ³ , 29,715.8 kcal/kgmole							

**Fig. 3. The drawing of heat & mass balance of each pipe in case 4.**

was considered to occur uniformly. To meet the value of GHSV, the inner volume of the catalyst layer was calculated. For sufficient mixing of the fuel and the oxidant, the space corresponding with that of the catalyst layer immediately above that layer was needed. Below the layer, some space was also made. In order to diffuse the fuel evenly, regular holes were made in each pipe for hydrogen and natural gas and each pipe for anode off and cathode off gas recycled, as shown in Fig. 2. As expressed in Fig. 2, there are five 2-mm holes in each hydrogen and natural gas pipe and twenty two 10-mm holes in each pipe of anode off gas and cathode off gas recycled. Even though the fuel was just a little mixed with other gases in actual operation, the gases did not flow uniformly. It was concluded that the non-uniform temperature distribution in the catalytic combustor could be primarily attributed to the asymmetric shape of the com-

Table 2. Gas compositions of each pipe in Fig. 3

Pipe no.	1	2	3	4	5
CH ₄		0.0200			
CO		0.1210	0.0000		
CO ₂	0.0429	0.5140	0.1184	0.0003	0.0790
H ₂		0.3090	0.0000		
H ₂ O	0.0247	0.0360	0.0691	0.0101	0.0370
N ₂	0.7973		0.7212	0.7729	0.8180
O ₂	0.1309		0.0874	0.2075	0.0660
Ar	0.0042		0.0038	0.0092	
Avg. molemass (kg/kmole)	29.03	27.60	29.61	28.85	29.17
LHV (kJ/mol)	0.00	125.01	0.02	0.00	0.00
HHV (kJ/mol)	0.00	140.36	0.02	0.00	0.00

busion space. The flow path and temperature distribution of the gases into the combustor in the operating conditions of case 4 were simulated and are shown in Fig. 4.

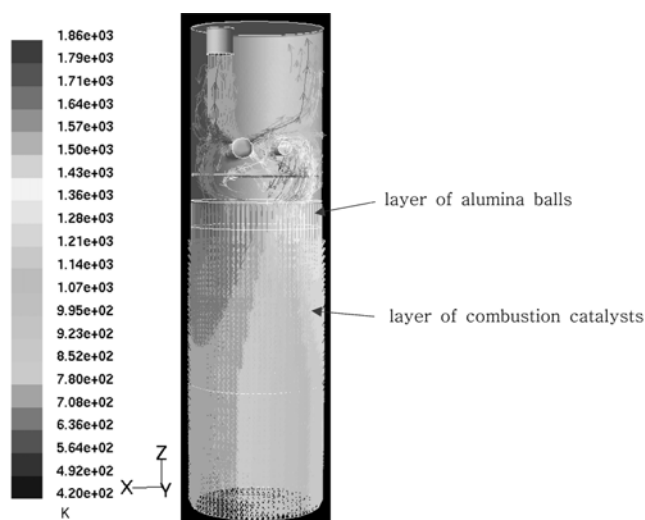
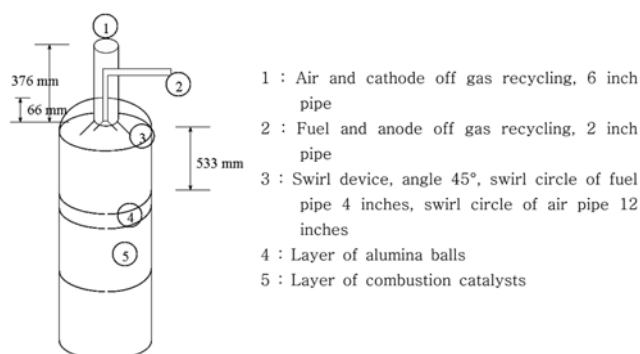
The existence of hydrogen in the anode off gas resulted in a high temperature, 1,860 K, around the pipe (pipe number 13 in Fig. 2) for the anode off gases. In the catalysts, the temperature distribution was very broad, from 636 to 1,360 K; this is also attributed to the asymmetric structure of the inner space of the combustor. Without sufficient mixing of the cathode off gases and anode off gases, a large amount of cathode off gases as well as anode off gases are transferred directly down. The temperatures around the anode off gases are higher than those around the cathode off gases, owing to the existence of abundant fuel. As noted above, the highest temperature was roughly 1,860 K, which led to cracking of the combustor

Table 3. The reactions and their rate coefficients

Reaction eq.	Arrhenius reaction rate coefficients		Reacting position
	Pre-exp. factor, A (s ⁻¹)	Activation energy, E (J/kgmole)	
CH ₄ +1.5O ₂ →CO+2H ₂ O	5.012×10 ¹¹	2×10 ⁸	Gas chamber zone
CO+0.5O ₂ →CO ₂	2.239×10 ¹²	1.7×10 ⁸	Gas chamber zone
CH ₄ +2O ₂ →CO ₂ +2H ₂ O	1×10 ¹⁵	1×10 ⁶	Catalyst zone
H ₂ +0.5O ₂ →H ₂ O	9.87×10 ⁸	3.1×10 ⁷	Gas chamber and catalyst zone

Table 4. Specifications of the catalyst in the catalytic combustor

Catalyst type	Pd type oxidation catalyst	
Properties	Shape, size	Spheres, 2-4 and 4-6mm Diameter
	Bulk density	0.8-1.0 kg/L
	Composition	Pd 0.28%, Al ₂ O ₃ balance
Operating condition	Temperature (°C)	400-1,100
	Pressure	more than Ambient
	GHSV (hr ⁻¹)	5,000-50,000

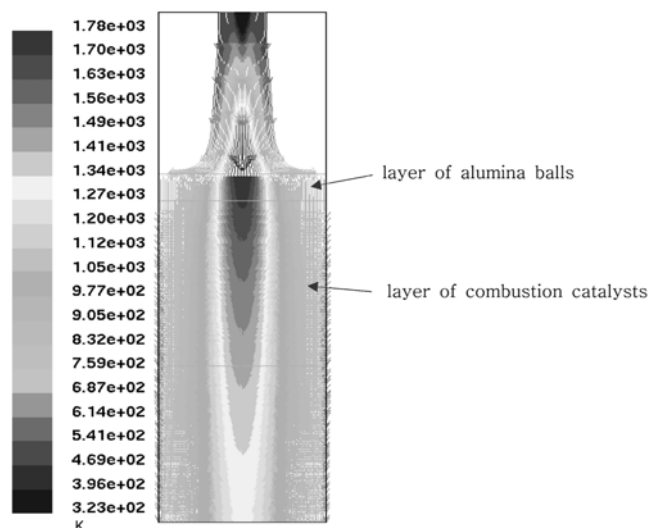
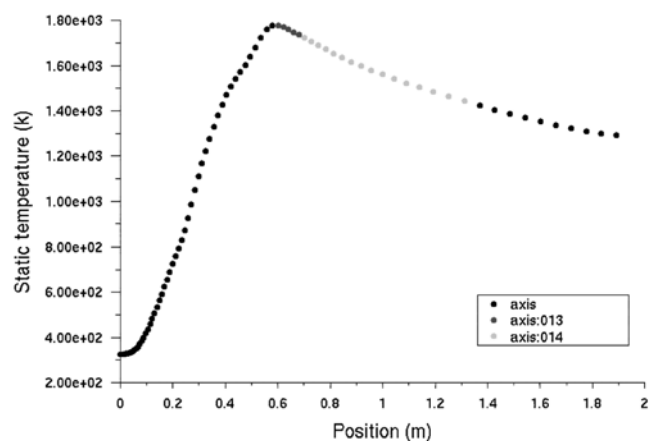
**Fig. 4. Flow path and temperature distribution of the gases in combustor (operating conditions: case 4).****Fig. 5. Shape of the revised catalytic combustor.**

wall. Therefore, instead of the asymmetric inner structure of the catalytic combustor, a symmetric structure has been considered.

2. CFD Analyses of the Revised Catalytic Combustor

2-1. CFD Analysis without Swirl

A CFD analysis of the existing catalytic combustor verified that the asymmetric inner structure cannot distribute the temperatures uniformly; thus, a symmetric structure is proposed. The revised shape of the catalytic combustor is depicted in Fig. 5. Details of the inner structure are provided in Fig. 5. The anode off gases and fuel such as hydrogen and natural gas are introduced into the pipe denoted as number two in Fig. 5. The cathode off gases and fresh air pass through pipe number one. The CFD analysis was performed in an

**Fig. 6. Flow path and temperature (K) distribution of the gases in the revised structure without a swirl device.****Fig. 7. Variation of temperature along the length at the center at the conditions of case 4 in the revised structure without a swirl device.**

axisymmetric, two-dimensional, steady state [8]. Because the structure of the inner space of the combustor is symmetric, the CFD analyses should show the same results at any two-dimensional face vertically cutting the center of the combustor.

First, the swirl device was not used. As a result, the heat concentrated on the center of the combustor, as shown in Fig. 6. The highest temperature was 1,780 K at the point reaching alumina balls which were used for dispersion. The lowest temperature, 687 K, was meanwhile measured near the wall of the combustor. A graph showing the variation of temperature along the length from top to bottom in the center of the combustor is presented in Fig. 7. In Fig. 7, the dots described as “axis” indicate the values from the top to alumina ball layer, “axis:013” is the temperature values in the layer of alumina balls, “axis:014” is those in the catalysts, and black dots indicate the region beyond the catalysts.

Through the CFD analysis, it was estimated that as the overall flow passes by the center of the combustor, only the catalysts around the center region play a role and those near the wall do not. In order

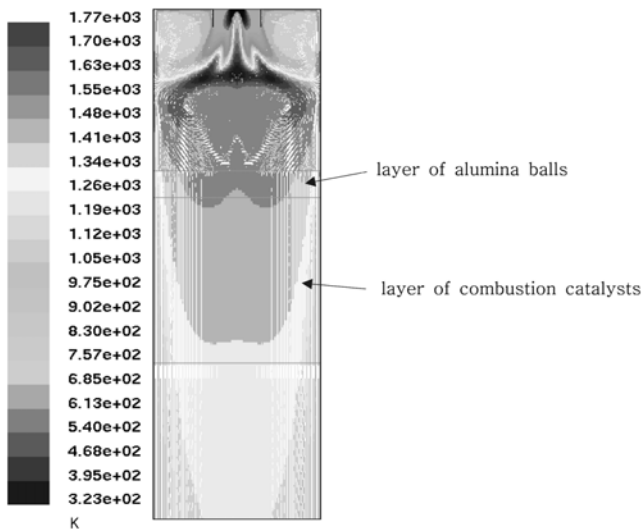


Fig. 8. Flow path and temperature (K) distribution of the gases in the revised structure with a swirl device at an angle of 45°.

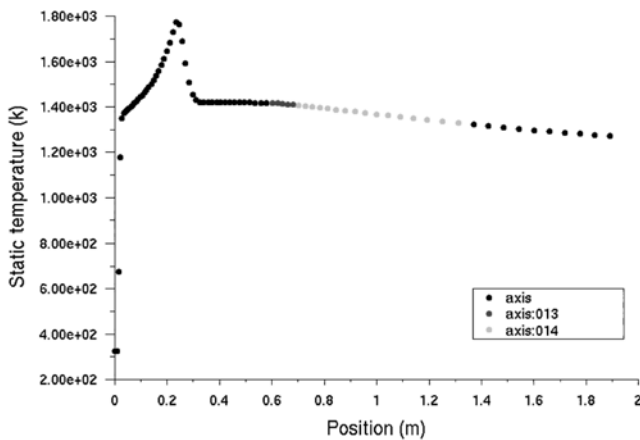


Fig. 9. Variation of temperature according to the length at the center at the conditions of case 4 in the revised structure with a swirl device (swirl angle 45°).

to utilize the whole space of the combustor, it appears the injected gases should be subjected to a swirl device.

2-2. CFD Analysis of the Revised Catalytic Combustor Considering Swirl

The results of the CFD analysis are presented in Figs. 8 and 10. The angle of the swirl device is 45° in Fig. 8 and 20° in Fig. 10. With swirling of the injected gases, the range of temperature for the catalysts narrows from 1,100 K to 1,400 K and it appears that all of the catalysts are used. The highest temperature in the inner combustion space is 1,770 K in Fig. 8 and 1,750 K in Fig. 10, near the swirl device. Graphs showing the temperatures along the length from top to bottom in the center of the combustor are presented in Figs. 9 and 11, respectively. For a swirl angle of 20°, the highest temperature was measured near the top, that is, near the swirl device, and for an angle of 45°, the highest temperature was found slightly farther from the top. These temperatures would result in fatal damage to the surface of the swirl device. Therefore, a heatproof coating should be applied to the surface of the swirl device for protection.

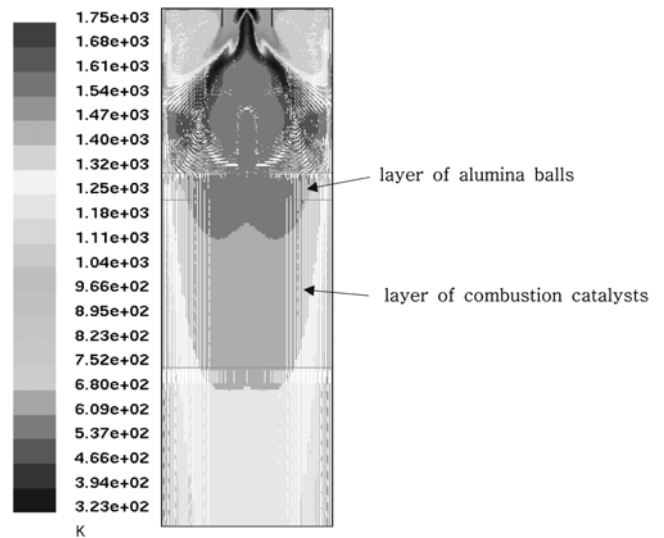


Fig. 10. Flow path and temperature (K) distribution of the gases in the revised structure with a swirl device at an angle of 20°.

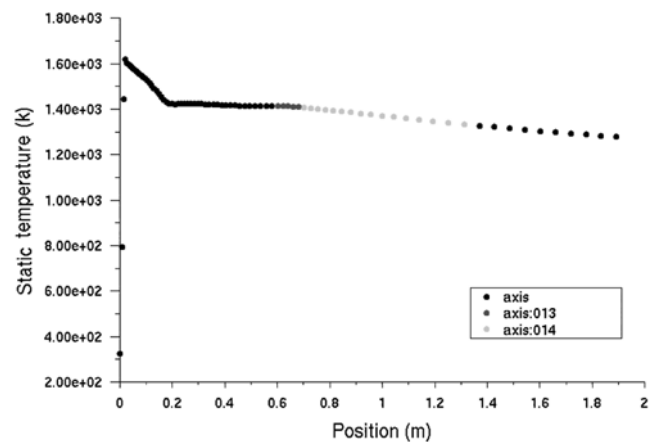


Fig. 11. Variation of temperature according to the length at the center at the conditions of case 4 in the revised structure with a swirl device (swirl angle 20°).

Compared with Fig. 8 and 10, it is found that the shape of the flame in Fig. 8 with a swirl device angle of 45° is greater in width and shorter in length than that in Fig. 10. In the combustor dimensions of this study, the temperature near the wall of the combustor appears to be lower in the case showing in Fig. 10 than that in Fig. 8, and thus a lower angle is preferable for the swirl device.

Because the temperature near the wall influences the durability of the material of the wall, it is important to determine the optimal angle of the swirl device.

By virtue of these simulations, it is estimated that as the diameter of the combustor becomes larger, the angle of the swirl device should also be increased.

2-3. CFD Analysis of the Revised Catalytic Combustor using Hydrogen and Natural Gas

At the initial start-up of the catalytic combustor, because the anode off gas and cathode off gas are not used and hydrogen is used up to 400 °C and then natural gas is employed up to 600 °C, the combus-

tion tendencies of hydrogen and natural gas should be studied.

The lower heating value of hydrogen is 57,364 kcal/kgmol and that of natural gas is 190,515 kcal/kgmol. The calorie of natural gas is over 3 times higher than that of hydrogen. Therefore, if same volume of each hydrogen and natural gas is burned, the temperature of the combustor will be higher in a combustor burning natural gas. In the existing combustor, this tendency was observed for the combustion conditions of cases 1 and 2 shown in Table 1.

As another tendency, as mentioned in the paper of Sadamori [9], NG cannot burn more easily than hydrogen at low temperature either. In the revised combustor without a swirl device, the natural gas, that is, in the conditions of case 2, was not burned in the simulation. The initial methane volume was regarded as 2.5%, compared with the overall gases, and the methane fraction at the outlet of the combustor at the end of the simulation was also the same. The graph of the variation of methane fraction along the length from top to bottom in the center of the combustor is shown in Fig. 12. Even if the natural gas was heated to 280 °C and the air to 400 °C, very little natural gas was burned. The methane fraction at the outlet of the combustor was calculated to be 1.4% in the case of heating NG up

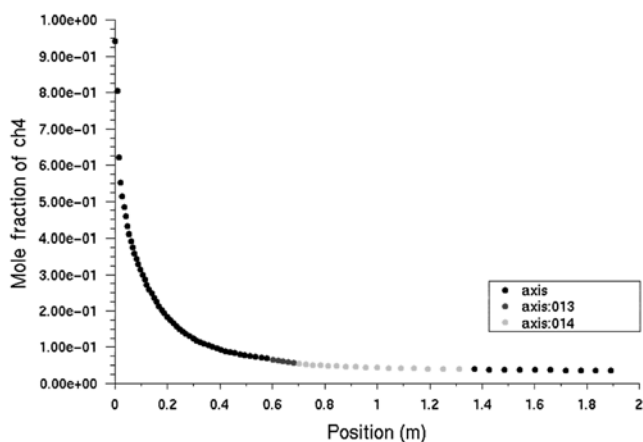


Fig. 12. Mole fraction of CH_4 according to the length at the center at the conditions of case 2 in the revised structure without a swirl device.

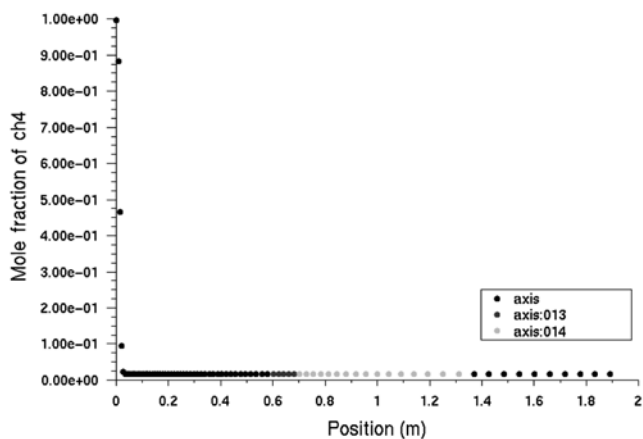


Fig. 13. Mole fraction of CH_4 according to the length at the center at the conditions of case 2 in the revised structure with a swirl device.

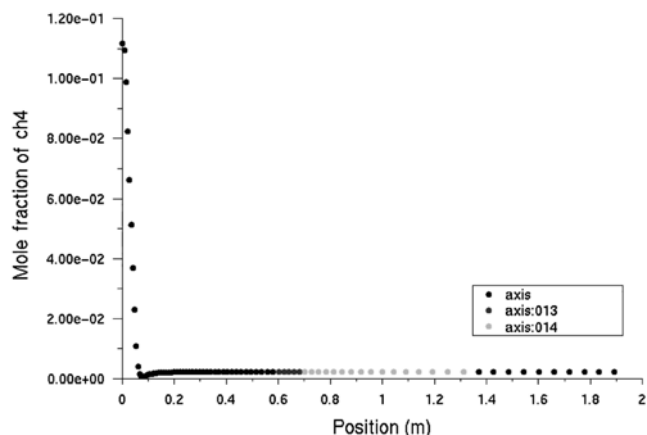


Fig. 14. Mole fraction of CH_4 according to the length at the center at the conditions of case 3 in the revised structure with a swirl device.

to 280 °C and 2.2% in the case of heating air up to 400 °C.

Notably, when a swirl device was used, the combustion was improved. For the combustion of case 2 in the revised combustor with a swirl device, the concentration of unburned methane at the outlet of the combustor was 1.6% as the ratio of volume, which corresponded to 34.8% combustion of the total methane. The methane fraction at the center of the combustor is shown in Fig. 13. When the swirl device is applied, the combustion reaction takes place fully near the swirl device, as shown in the same figure.

However, in the condition of case 3, where hydrogen and natural gas are burned together, the unburned methane at the outlet of the combustor was estimated to be 0.2% as the ratio of volume, which corresponded to 91.7% combustion, compared with total injected gases. The methane fraction at the center of the combustor is shown in Fig. 14.

When comparing the cases without a swirl device, shown in Fig. 12, with those where the swirl device is applied, shown in Figs. 13 and 14, a high methane fraction was found at any distance from the top. It is assumed that little diffusion occurred in the case without a swirl device. Proceeding down, the methane is diluted with the air and the fraction becomes low but the methane is not burned.

In the CFD analysis results, compared to hydrogen, NG does not readily burn at low temperature. Through the CFD analysis, the combustion of natural gas at various conditions should be estimated through simulations.

CONCLUSIONS

In order to determine the cause of rupture of the catalytic combustor wall during the initial start-up of the combustor, analyses of the computational fluid dynamics of the existing combustor and proposed types were performed. The fracture of the wall was attributed to be the asymmetric inner structure of the combustor.

In the revised combustor type having symmetric structure without a swirl device, the flow of gases was concentrated on the center of the combustor. Thus, only catalysts around the center region were used according to the simulation. When the revised combustor of the symmetric structure with a swirl device was simulated, the overall temperatures were found to be uniform. However, near

the swirl device, high temperature exceeding 1,700 K was measured. Therefore, a heatproof coating of the surface of the swirl device should be applied.

At the initial start-up of the catalytic combustor, the hydrogen and natural gas were used. In the case where only natural gas was used, the gas did not burn in the revised combustor without a swirl device according to the simulation. Meanwhile, in the combustor with the swirl device, methane of 34.8% volume was simulated to be burned. However, when hydrogen and natural gas were burned together, methane of 91.7% volume was burned in the simulation.

As results of CFD analyses, the symmetric inner structure in the catalytic combustor would be preferable to the asymmetric one which produced non-uniform gas flows. Also, a combustor using a swirl device would be effective to utilize catalysts uniformly. Because hydrogen burns more easily than NG, NG mixed with hydrogen would be apt to burn more easily than when burning only NG.

ACKNOWLEDGMENTS

The development of this catalytic combustor is a part of the project "The development of a 100 kW class externally reformed molten carbonate fuel cell." Financial support for this project was provided by the Korea Energy Management Corporation and the Electric Power Industry Technology Evaluation & Planning. The Korea Electric Power Research Institute would like to express its appreciation for the support of these fine organizations.

NOMENCLATURE

ρ : density [kg/m³]
 v : velocity [m/s]

v_{mag} : velocity magnitude [m/s]
 v_i : i-direction velocity [m/s]
 ∇p : pressure drop [Pa]
 g : gravity [m/s²]
 S : source term
 μ : viscosity of the fluid [kg/m·s]
 α : permeability [m²]
 C_2 : inertial loss factor of the porous media [1/m]
 D_p : diameter of the catalyst [m]
 ε : void fraction, defined as the volume of voids divided by the volume of the packed bed region

REFERENCES

1. G. Groppi, E. Tronconi, P. Forzatti and M. Berg, *Catalysis Today*, **59**, 151 (2000).
2. Y.-S. Seo, S.-K. Kang, M.-H. Han and Y.-S. Baek, *Catalysis Today*, **47**, 421 (1999).
3. K. W. Beebe, K. D. Cairns, V. K. Pareek, S. G. Nickolas, J. C. Schlatter and T. Tsuchiya, *Catalysis Today*, **59**, 95 (2000).
4. FLUENT 6.2 User Guide, FLUENT Inc. (2003).
5. B. E. Launder and D. B. Spalding, *Lectures in mathematical models of turbulence*, Academic Press, London, England (1972).
6. B. F. Magnussen and B. H. Hjertager, *On mathematical models of turbulent combustion with special emphasis on soot formation and combustion*, In 16th Symp. (Int'l) on Combustion. The Combustion Institute (1976).
7. S. Ergun, *Chem. Eng. Prog.*, **48**(2), 89 (1952).
8. Y.-S. Seo, K.-S. Song and S.-K. Kang, *Korean J. Chem. Eng.*, **20**, 819 (2003).
9. H. Sadamori, *Catalysis Today*, **47**, 325 (1999).